Optical Properties of Surfaces Covered with Latex Particles: Comparison with Theory

ARTICLE *in* THE JOURNAL OF PHYSICAL CHEMISTRY · JANUARY 1995

Impact Factor: 2.78 · DOI: 10.1021/j100002a049

5 AUTHORS, INCLUDING:

Ger Koper
Delft University of Technology
157 PUBLICATIONS **2,693** CITATIONS
SEE PROFILE

Dick Bedeaux
Norwegian University of Science and Technol…
305 PUBLICATIONS **5,551** CITATIONS
SEE PROFILE

Optical Properties of Surfaces Covered with Latex Particles: Comparison with Theory

Elizabeth K. Mann,[†] Erik A. van der Zeeuw,*[,‡] Ger J. M. Koper,[‡] Pierre Schaaf,[†,§] and Dick Bedeaux[‡]

Institut Charles Sadron (CNRS-ULP), 6 rue Boussingault, 67083 Strasbourg, France, Department of Physical and Macromolecular Chemistry, Leiden University, Gorlaeus Laboratories, P.O Box 9502, 2300 RA Leiden, The Netherlands, and Ecole Européene de Hautes Etudes des Industries Chimiques de Strasbourg, 1 rue Blaise Pascal, 67000 Strasbourg, France

Received: August 17, 1994[⊗]

Scanning-angle reflectometry around the Brewster angle has been used to investigate the optical properties of positively charged polystyrene particles with radii ranging from 50 to 500 nm, deposited on a silica/water interface. A theory for inhomogeneous thin films may be used to analyze the data for the smallest of these particles, but gives incorrect results for the larger ones. A model based on Mie theory describes the data well over the entire size range. This model ignores direct particle substrate interactions, which is justified for the small differences in refractive indices in this system. It is shown that the Mie-based model is equivalent to the thin film model in the long-wavelength limit. The analysis yields three parameters: particle size, refractive index, and coverage.

1. Introduction

The adsorption of colloidal particles at a liquid/solid interface has received considerable theoretical attention in the last decade,[1] serving as a model system for situations of practical importance such as the fouling of filtration devices and the adsorption of bacteria on biomaterials. Only few experimental studies are available.[2,3] Recent microscopic studies of large particles (>2 μm)[4] adsorbing on surfaces have fruitfully tested the applicability of various theoretical models. In order to study the deposition of smaller particles, with different transport properties in the bulk liquid, other methods must be used.

Scanning-angle reflectometry[5] is one method adapted for the study of interfaces. The technique uses the special properties of the reflectivity of polarized light around the Brewster angle: the reflectivity of light polarized parallel to the incident plane (polarization p) is zero at this angle for a perfectly abrupt, smooth (i.e. Fresnel) interface. In the presence of an interfacial layer, the reflectivity at the Brewster angle is no longer zero: the minimum reflectivity increases, the angle at which this minimum is observed shifts away from the Brewster angle, and the shape of the reflectivity curve as a function of angle alters (see Figure 3). The reflectivity around the Brewster angle is thus very sensitive to the character of the interfacial region.

It is the purpose of this work to investigate the utilization of this method to study colloidal latex particles (radius 50-500 nm) deposited at the glass/water interface, in the context of optical theories applicable to inhomogeneous thin films. This also allows us to test these theories extensively, in the limit applicable to dielectric systems with only *small* differences between the various refractive indices.

The optical properties of particles in free space have been the subject of research for more than a century. Three different situations can be distinguished: (1) the particles are much smaller than the wavelength of the incident light, (2) they are comparable, or (3) they are much larger than the wavelength. In situation 1, the incident electromagnetic fields can be assumed to be homogeneous in the neighborhood of the particles, and one can use the dipole approximation, or Rayleigh theory. In situation 3, geometric optics can be applied to determine the optical properties. Situation 2 is the most difficult since no *a priori* approximations can be made. A general approach is required that includes both situations 1 and 3 as limiting cases. For isolated spheres this is given by Mie theory.[6,7]

For particles on a surface, the problem is even more complicated: the electromagnetic interaction between the particles and the substrate may play an important role. Again one can distinguish between situations 1, 2, and 3 mentioned above and attempt to determine the optical properties for a given shape of particle. Several forms of small particles have been considered: pits and bumps in a substrate,[8] hemispheres,[9] spheres,[10] truncated spheres,[11,12] and spheroidal particles.[13] Bobbert et al. have developed the general theory for arbitrarily sized spheres on a substrate.[14,15] It is in general also important to take the interaction between the particles into account. For particles that are small compared to the wavelength of light, Vlieger and Bedeaux have developed a theory to do this in the dipole approximation.[16] This analysis was extended by Haarmans and Bedeaux to arbitrary order in the multipole approximation.[17,18] Qualitative agreement has been found between these theories and a limited number of experiments, such as the single-angle ellipsometry studies of Greef.[19] Many aspects of these theories remain to be tested, however.

The experiments reported here provide one stringent test of these theories, in the limit in which the differences between all dielectric constants are small, which allows us to ignore the interactions between the spheres and with the substrate. We show that in this case the optical theories can be rephrased to provide a numerically tractable test. In particular, we interpret the reflectivity as due to light reflected separately from the layer of spheres and the substrate, along with multiple reflections between the two. The interaction between the spheres in the layer is neglected for the low surface coverages observed.

In the next sections we will demonstrate how to obtain information on the size of the particles, as well as on the coverage and their refractive index. We demonstrate also the limits of the theory of thin inhomogeneous films and show that

[†] Institute Charles Sadron.
[‡] Leiden University.
[§] Ecole Européene de Hautes Etudes des Industries Chimique de Strasbourg.
[⊗] Abstract published in *Advance ACS Abstracts,* December 15, 1994.

0022-3654/95/2099-0790$09.00/0

satisfactory results over the entire size range can only be obtained using Mie theory.

2. Theory

The latex particles are modeled here as homogeneous spheres of radius a. We shall neglect size polydispersity, although it can easily be taken into account. The latex is nonabsorbing at the wavelength considered, so that its refractive index is real. The particles are located at the silica/water interface. Experimentally, we observed that this interface behaved like a perfect Fresnel interface.

In this section we will first consider the light scattered by an uncorrelated assembly of spheres, assumed to lie in a plane. The Fresnel interface is then introduced at a distance h from the center of the spheres. The analysis follows that of Bobbert et al.,[13] but simplifies considerably because (a) the differences between the refractive indices of the three media are small and (b) interactions between spheres can be ignored in the low-density limit. The expressions obtained will then be compared to existing expressions for inhomogeneous thin films, with film thicknesses d much smaller than λ, the wavelength of light in vacuum, corresponding to radii $a \ll \lambda$. This will allow us some evaluation of the limitations of the approach presented here.

First we discuss the spheres only, in the absence of a glass substrate. The light scattered by an isolated sphere is described by Mie theory.[6,7] Given an incident plane wave, electric field $\mathbf{E}_i = \exp\{i\mathbf{k}\cdot\mathbf{r}\}\mathbf{e}_i$. We shall be interested in light scattered in the plane determined by the wave vector $\mathbf{k}$ and the polarization vector $\mathbf{e}_i$. The scattered electric field due to one sphere is

$$E = \frac{e^{ik_2 r}}{ik_2 r} S_p(\theta) \tag{2.1}$$

where k_2 is the wavenumber $k_2 = 2\pi n_2/\lambda$, and n_2 the refractive index of the water. $S_p(\theta)$ is the scattering function for p-polarized light (see Appendix A) and depends on the scattering angle θ, the radius of the sphere, and the ratio of the refractive indices of the sphere and water. This function is written as a multipole expansion, where the first term corresponds to the scattering of the induced electric dipole. For small particles, of radius $a \ll \lambda$, only the dipole contribution is significant, and the scattering function is then given by

$$S_p(\theta) \simeq \frac{ik_2^3 \alpha \cos\theta}{4\pi n_2^2} \quad (a \ll \lambda) \tag{2.2}$$

where α is the polarizability of the spheres in the water,

$$\alpha = 4\pi a^3 n_2^2 \frac{n_3^2 - n_2^2}{n_3^2 + 2n_2^2} \tag{2.3}$$

Here n_3 is the refractive index inside the sphere. Equation 2.2 corresponds to the expression given by Rayleigh[6,7] for small particles.

Next, let us consider an assembly of spheres in a plane. At sufficiently low surface coverages, the electromagnetic interactions between the spheres and the resulting modification of the scattering function can be neglected. For such a layer, light is scattered coherently in the direction with scattering angle $\pi - 2\theta_2$, where θ_2 is the angle between the incident light beam and the normal of the plane. The angle of reflection is equal to the angle of incidence, as with a homogeneous slab. The total field coherently scattered by the layer of spheres and in the absence of a substrate has been calculated by Bobbert et al.,[15] yielding

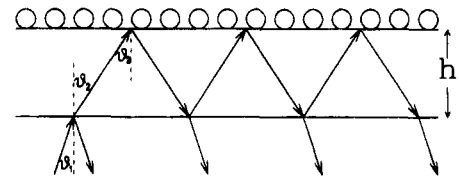

Figure 1. Light reflected from an assembly of noninteracting spheres placed randomly in a plane a distance $h \gg a$ above the substrate–ambient interface. The light, incident at angle θ_1, is refracted at the interface at angle θ_2. This light is scattered by the individual spheres; the only contribution which is scattered coherently between the spheres has a scattering angle $\pi - 2\theta_2$.

an amplitude reflection coefficient

$$r_f(\theta_2) = \frac{2\phi S_p(\pi - 2\theta_2)}{k_2^2 a^2 \cos\theta_2} \tag{2.4}$$

where ϕ is the surface coverage. For spheres that are sufficiently small, the dipole approximation eq 2.2 applies, and eq 2.4 reduces to

$$r_f(\theta_2) = -i\frac{\phi\alpha \cos 2\theta_2}{\lambda a_2 n_2 \cos\theta_2} \tag{2.5}$$

Now we introduce the glass substrate. For a pure silica/water interface, the amplitude reflection coefficient for p-polarized light is given by the Fresnel expression

$$r_{12} = \frac{n_2 \cos\theta_1 - n_1 \cos\theta_2}{n_2 \cos\theta_1 + n_1 \cos\theta_2} \tag{2.6}$$

where n_1 and n_2 are the refractive indices of the silica and the water, respectively. The angle θ_2 on the water side is related to the incidence angle θ_1 on the silica side by Snell's law: $n_1 \sin\theta_1 = n_2 \sin\theta_2$.

Let us now consider a layer of noninteracting spheres situated at a height h above the silica/water interface (see Figure 1). For h sufficiently large, the sum of the fields scattered by all the particles can again be approximated by a plane wave at the Fresnel interface. Moreover, the polarizabilities of the spheres will be nearly unchanged by the presence of the interface. The scattering function appearing in the amplitude reflection coefficient given by eq 2.4 then differs little from that for free spheres. The reflection coefficient for such a system can be found by summation over the contributions due to multiple reflections between the layer of spheres and the Fresnel surface, in the same way as for layered structures,[20] which gives

$$r = r_{12} + t_{12}r_f t_{21}e^{i\Delta} + t_{12}r_f r_{21}r_f t_{21}e^{2i\Delta} + t_{12}r_f r_{21}r_f r_{21}r_f t_{21}e^{3i\Delta} + \ldots$$
$$= \frac{r_{12} + r_f e^{i\Delta}}{1 + r_{12}r_f e^{i\Delta}} \tag{2.7}$$

where $\Delta = 2k_2 h \cos\theta_2$ is the phase difference between the field reflected at the interface and the light coherently scattered from the spheres. For distances h of the order of the radius of the spheres, the scattering function appearing in eq 2.1 is modified by the presence of the silica/water interface. However, due to the small difference between the refractive indices of silica and water, the modification of the scattering function in the present case is quite small. For the dipole contribution to the scattering function it is not more than 0.3% and will therefore be neglected.[11]

Expression 2.7 can be compared to three other expressions appearing in the literature. First we compare with the expression in ref 21. By expanding eq 2.7 in r_l and taking the absolute value squared, we find for the reflectivity

$$R \simeq r_{12}^2 + 2t_{12}t_{21}r_{12}\{\mathrm{Re}(r_l)\cos\Delta - \mathrm{Im}(r_l)\sin\Delta\} + t_{12}^2t_{21}^2|r_l|^2 - 2t_{12}t_{21}r_{12}^2\{\mathrm{Re}(r_l^2)\cos 2\Delta - \mathrm{Im}(r_l^2)\sin 2\Delta\} \quad (2.8)$$

The second term in the above expression is of order ϱ, whereas the last two terms are of order ϱ^2. The last term can even be neglected around the Brewster angle ($\theta_B - 3° \le \theta \le \theta_B + 3°$), because it differs by a factor $r_{12}^2 \le 10^{-6}$ from the term preceding it. Thus, we get a simple expression consisting of three terms, one due to reflection from the Fresnel interface, one due to scattering from the particles, and finally one due to interference between these two contributions:

$$R \simeq r_{12}^2 + 2t_{12}t_{21}r_{12}\{\mathrm{Re}(r_l)\cos\Delta - \mathrm{Im}(r_l)\sin\Delta\} + t_{12}^2t_{21}^2|r_l|^2 \quad (2.9)$$

This is the expression given in ref 21. See ref 22 for a clarification of apparent differences.

In the case of small particles, for which one may approximate $\exp(i\Delta) \simeq 1 + i\Delta$, eq 2.7 reduces to the one developed by Vlieger and Bedeaux for thin island films,[16] where the reflection coefficient has the form

$$r_l = -\frac{i\pi}{\lambda}\left\{\frac{\frac{\gamma\cos\theta_2}{n_2}}{1-\frac{i\pi}{\lambda}\frac{\gamma\cos\theta_2}{n_2}} - \frac{\frac{\beta n_2 n_1^2\sin^2\theta_1}{\cos\theta_2}}{1-\frac{i\pi}{\lambda}\frac{\beta n_2 n_1^2\sin^2\theta_1}{\cos\theta_2}}\right\} \quad (2.10)$$

Here, γ and β are the surface excess dipole polarizabilities parallel and perpendicular to the interface. For small spheres at low surface coverages ϕ, these constitutive coefficients are given by Haarmans[17]

$$\gamma = n_2^4\beta = \phi\alpha/\pi a^2 \quad (2.11)$$

Substituting these expressions for γ and β in eq 2.10 indeed yields the reflection coefficient for a layer of small particles, cf. eq 2.5.

The two terms in eq 2.10 are easily understood in terms of the response of the media to projections of the incident electric field in the directions parallel and perpendicular to the interface. The denominators originate in the dynamic contributions from the field scattered by the particles: the particles respond not simply to the incident field but rather to the *local* field, which is the sum of the incident field and the field produced by all the other particles. The static contribution, which is independent of the angle of incidence, is included in the effective polarization densities γ and β. An explicit calculation of the local field is presented in Appendix B. In the limit in which the refractive indices of the substrate and ambient media are close, the presence of the Fresnel interface can be neglected.

We see that for low coverage, when local field effects are negligible, eq 2.10 corresponds to eq 2.5, which originated from the Mie-based theory. This gives us some indications of the limitations of this theory, at least as it applies to small spheres. For the refractive indices encountered here, the local field corrections are on the order of $\pi\gamma/\lambda n_2 \approx 2\phi a/\lambda$. As ϕ increases, the polarizabilities β and γ are also modified due to the static contribution of the local fields (see Appendix B), but only by relative corrections on the order of 0.1ϕ, for the particular media encountered here (with comparable values for all refractive indices).

The Vlieger/Bedeaux expressions (eq 2.7 with 2.10) can be expanded to second order in β and γ, to give a simple linear form:[23]

$$R \simeq r_{12}^2 - 2t_{12}t_{21}r_{12}(J_{21} - n_1^2\sin^2\theta_1 J_{22}) + t_{12}^2t_{21}^2\frac{n_1\sin^4\theta_1}{4n_2^3\cos\theta_1\cos\theta_2}J_1^2 \quad (2.12)$$

where the constants are given by

$$J_1 = \frac{2\pi}{\lambda}(\gamma - n_1^2n_2^2\beta)$$

$$J_{21} = \left(\frac{2\pi}{\lambda}\right)^2\left(\tau + \frac{1}{2(n_1^2 - n_2^2)}\gamma^2\right) \quad (2.13)$$

$$J_{22} = \left(\frac{2\pi}{\lambda}\right)^2\left(\delta + \frac{n_1^2 + n_2^2}{2(n_1^2 - n_2^2)}\gamma\beta\right)$$

where $\tau = -\gamma a$ and $\delta = 2\tau/n_2^2$ at low coverages.

The constitutive coefficients β, γ, τ, and δ are the excess dipole and quadrupole polarizabilities of the spheres with respect to the surface of the substrate. It is noted that if one chooses a different surface with respect to which one calculates the excess dipole and quadrupole polarizabilities, one finds different values for these quantities and, as a consequence, for β, γ, τ, and δ. Since the reflectivity of the real interface cannot depend on the position of this fictitious interface, only *invariant* combinations of these coefficients can appear in the multiple expansion of this reflectivity given by eqs 2.12 and 2.13. Comparison with formulas derived by Bedeaux/Vlieger[23] and by Lekner[24] shows that the constants J_1, J_{21}, and J_{22} are dimensionless forms of these *optical invariants*. For more details on these optical invariants, refer to Appendix C.

We will compare our data with the two linear forms, eq 2.9 with eq 2.4 (referred to as the "Mie-based theory"), and for smaller spheres to eq 2.12 (the "invariant" or "Bedeaux/Vlieger" formulation). For the Mie-based theory, the radius is a sensitive fitting parameter, and agreement between the deduced values and those provided by the manufacturer is a critical test of the validity of the model. For the invariant formulation, the size can be deduced from the ratio of the second-order and the first-order invariants. For low surface coverages ϕ, we expect from eqs 2.11 and 2.13

$$J_{21}/J_1 = \left(\frac{2\pi}{\lambda}\right)an_2^2/(n_1^2 - n_2^2) \quad (2.14)$$

Further, for these low coverages the ratio of the two second-order invariants should be proportional to the refractive index of the medium surrounding the particles,

$$J_{21}/J_{22} = n_2^2/2 \quad (2.15)$$

The values for these ratios thus provide tests for the applicability of the model to the given experimental situation.

3. Experimental Methods

Adsorption was performed onto the optically flat hypotenuse of a rectangular prism made of quartz (Suprasil, Heraus,

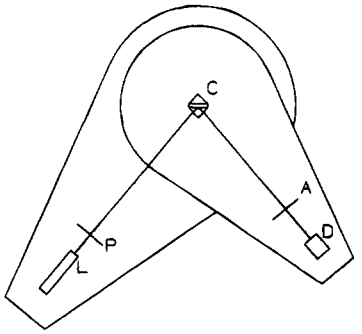

Figure 2. Schematic diagram of the reflectometer: (L) light source; (P), (A) polarizers aligned in the plane of incidence; (C) prism and sample cell, (D) photodetector.

refractive index $n = 1.457\ 18$) or glass (Schott BK 7, refractive index 1.515 09). Two prisms were mounted in a holder, leaving a 3 mm spacing between the two hypotenuse faces.

The method consists of measuring the reflection coefficient for p-waves at a number of angles around the Brewster angle (see Figure 2). The light source (L) is a 5 mW HeNe laser operating at a wavelength $\lambda = 632.8$ nm. Light passes through a polarizer (P), aligned in the plane of incidence, perpendicular to the adsorption surface. Along the path to this surface, the light passes almost perpendicularly through the entrance face of the prism (C). After reflection it leaves the prism through its exit face, passes through a second polarizer (A) that again selects the p-wave, and impinges on the photodetector (D). The reflectometer is fully automated and computer-controlled. We report results from two different instruments, one at the Institute Charles Sadron in Strasbourg (France) and one at Leiden University (the Netherlands). The French version of the instrument is horizontal. The adsorption surface is vertical, the laser is held fixed, and the angle of incidence is selected by rotating the cell by means of a high-precision goniometer; the position of the photodetector is adjusted to find the maximum in the reflected intensity. Further details may be found in ref 21. The Dutch version of the instrument is similar but oriented vertically. The adsorption surface was *chosen* to be horizontal. The angle of incidence is selected by simultaneously rotating the laser and the detector supports.

The measured intensities are related to the reflectivity $R_p(\theta_1)$ by

$$I(\theta_1) = I_0 + A\,R_p(\theta_1) \tag{3.1}$$

where I_0 is the residual intensity at the Brewster angle for a perfect interface and A is an instrument-dependent constant. The Brewster angle for the silica/water interface (used in Strasbourg) is about 42.5, while the Brewster angle for the glass/water interface (used in Leiden) is about 41.3. The amplitude reflection coefficient for a simple interface is given by the Fresnel expression (2.6).

At the beginning of each experiment, the reflected intensities I of the silica/water interface were measured for incidence angles θ_1 ranging from about 40° to 45°. This allowed us to determine the amplification of the signal, as well as the residual intensity at the Brewster angle.

The latex suspension was then introduced into the cell, and similar intensity curves were measured at about 10 min intervals. Typical curves are shown in Figure 3. The reflected intensity evolved with time at a rate depending on the concentration of the latex solution. The experiment ran, depending on the experiment, for 10 to 48 h. We flushed with water at the end of each experiment. Since the curves did not change significantly after that, we conclude that only adsorbed particles contributed to the evolution in reflected intensity. Data were stored in the computer for subsequent off-line analysis. The measurements were first corrected for transmission through the prism.

TABLE 1: Radius, Polydispersity, and Surface Charge Provided by the Manufacturer and Experimental Values[a]

a (nm)	σ (μC/cm^2)	a_{exp} (nm)	ϕ	χ/χ_f	loc
		61 ± 2	0.09	1.3	S
58 ± 11.7%	8.1	†42 ± 2	0.12	2.0	S
		53 ± 2	0.08	1.8	L
		†49 ± 1	0.12	1.6	L
67 ± 10.9%	8.2	71 ± 1	0.09	1.6	L
		†55 ± 5	0.13	2.0	L
96 ± 3.0%	4.3	99 ± 1	0.11	3.0	L
150 ± 3.3%	15.7	144 ± 1	0.13	1.4	S
		144 ± 2	0.11	1.8	L
239 ± 9.9%	11.0	240 ± 1	0.09	0.7	L
240 ± 7.0%	15.9	258 ± 2		1.0	S
300 ± 6.3%	9.8	325 ± 2	0.11	0.9	S
		325 ± 1	0.07	1.9	L
345 ± 9.5%	15.3	373 ± 1	0.09	5.1	L
381 ± 3.1%	12.9	410 ± 1	0.05	2.8	L
477 ± 4.1%	21.4	524 ± 1	0.04	5.0	L

[a] The error estimates on a_{exp} refer to the variation in time and between experiments: They indicate the sensitivity of the fitting procedure to this parameter. Note that χ is normalized to the χ_f of the Fresnel curve. The † indicates parameters obtained using eq 2.12 rather than eq 2.9. The last column shows where the experiment was done: Leiden or Strasbourg.

For the latex particles, we used polystyrene beads commercially available from Interfacial Dynamics Corp. (Portland, OR). Particles with positively charged amidine groups were chosen in order to ensure adsorption on the negatively charged surface. The particle solutions were diluted in pure water to concentrations ranging from 10^{-2} to 10^{-3}%. A range of different sizes, given in Table 1, were studied. The refractive index of the spheres is given as 1.591 (at 590 nm) by the manufacturer.

The different elements of the cell were cleaned with a laboratory-use detergent (Hellmanex II; Hellma GmbH D-7840 Mullheim) and rinsed copiously with deionized SuperQ-Millipore water (used throughout the experiment), a dilute sulfuric acid solution, and again water.

4. Results and Discussion

Examples of the angular dependence of the surface reflectivity are presented in Figure 3. Similar measurements were performed on a series of latex particles with radii ranging from 50 to 500 nm (see Table 1). In the presence of the latex particles, the minimum of the reflectivity may both shift and increase; one effect or the other may dominate depending on the particle size. The shape of the curve, most noticeably its width, also changes.

Attempts were made to fit these data to the two models discussed previously (eqs 2.9 and 2.12). Both of these models assume the absence of any particle correlation of scale significant with respect to the wavelength of light and that the particles are monodisperse, spherical, and rest directly on a perfect, planar surface. Within these limitations, the formulation in terms of invariants, eq 2.12, is expected to be valid if the spheres are of radius $a \ll \lambda$. For the lowest sphere radii ($a = 58$ and 67 nm) this might be expected to hold reasonably well ($\lambda/a \approx 8$). The Mie-based model eq 2.9 is valid for all sizes *if* the interactions between the spheres and between the spheres and the substrate can be neglected.

The fits to the Mie-based model were performed with the particle radius a and coverage φ as free variables. The results

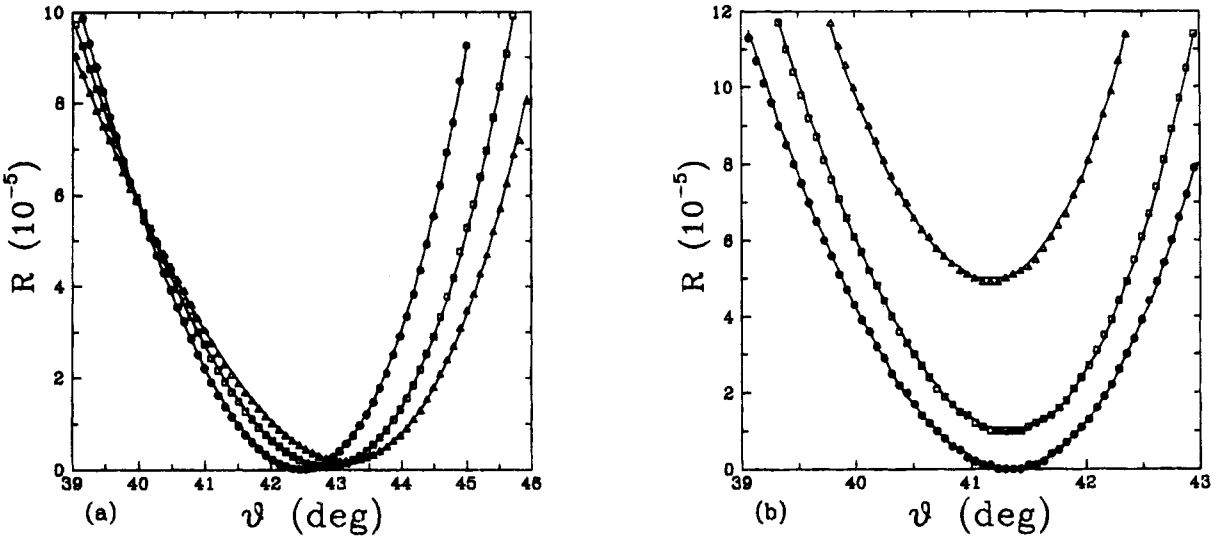

Figure 3. Reflectivity as a function of angle, before (solid symbols) and after (open symbols) injection of a solution of latex particles at time t = 0. Fits are done to the Mie-based model: (a) particles with radius a = 58 nm; (b) particles with radius a = 239 nm.

were rather insensitive to the remaining parameter n_3 (the refractive index of the spheres) within the range 1.58−1.62. It was therefore held fixed at the value given by the manufacturer (n_3 = 1.591). The fits were performed both directly with eq 2.9 and with the form which introduces two independent constants, c_1 and c_2:

$$R = r_{12}^2 + 2c_1 t_{12} t_{21} r_{12}\{\mathrm{Re}(r_l)\cos\Delta - \mathrm{Im}(r_l)\sin\Delta\} + c_2 t_{12}^2 t_{21}^2 |r_l|^2 \quad (4.1)$$

This provided a test of our assumption in using eq 2.9, for the Mie-based theory would predict $c_1^2/c_2 = 1$, if particle interactions can indeed be neglected. The more extended multiple-reflection formula, eq 2.7, was also used to fit the data, but corrections appeared to be negligible as expected for the angular range explored here.

In general we see good agreement between the experimental data and the Mie-based fits. The radius deduced from these Mie fits was essentially independent of time and surface coverage; see Figure 4. The radius, as well as the final surface coverage are given in Table 1. A measure of the quality of the fits is also given, by the average deviation χ between the experimental data and the fitted curves, normalized to the deviations observed for the Fresnel curves. In general, we see good agreement between the experimental data and the Mie-based fits. Some exceptions may be noted, in particular for the spheres of radius 96 nm and in some runs for the 58 nm spheres. Extensive particle aggregation was noted for these particular cases, in which case the models will not apply. We might note that the surface charge of the 96 nm particles was particularly low, which may indeed cause the particles to aggregate.

In all cases, we see excellent agreement in the particle sizes deduced by the two different groups (in Leiden and Strasbourg) and good agreement with the values given by the manufacturer. We also note that if the parameters c_1 and c_2 are left free, the ratio c_1^2/c_2 is found to be close to 1 (within 5%). We conclude therefore that the models that neglect interparticle interactions are relevant to our system.

For the smaller particles (a = 58 and 67 nm), the invariant fits were also of reasonable quality, and the ratio between J_{21} and J_1 yielded a well-defined particle size. Theory predicts a linear relationship between J_{22} and J_{21}, which was confirmed by our experiments. For particles of radius a as small as 150 nm, this was no longer the case (see Figure 4). Furthermore, the fits then suggested unphysical refractive indices for the water, as high as 2. These situations are beyond the physical validity of the invariant model, which assumed $a \ll \lambda$. But even for the 58 nm particles, the deduced particle size is consistently low, by about 20%. Comparisons between the exact expression and the approximation in terms of invariants for uniform layers of similar dimensions suggest that deviations of this order are expected. These deviations can also be made clear if we calculate the expected reflectivity according to eq 2.9 using eq 2.4 and compare the results with the expected reflectivities obtained using the Rayleigh approximation (eq 2.5) and the invariant approach (eq 2.12); see Figure 5. It demonstrates the already significant deviations of the invariant formulas from the Mie-based theory for spheres of radii $a \geq 25$ nm, when using eq 2.12. The more extended form, eqs 2.9 and 2.5, follows the Mie equation over a larger size range.

We see that in fact the fits to the Mie-based theory are very sensitive to the particle radius (±2 nm, see Table 1). The reason for this can be seen from the variation in the position and the value of the reflectivity minimum (see Figure 5). One would therefore expect that the experimental curves would not be described by the (monodisperse) theoretical curves if size polydispersity is present in the samples. This polydispersity can easily be introduced into our equations. We have simulated curves with a polydispersity of several percent and fitted these to our formulas, which do not take polydispersity into account. The quality of the fits remains reasonable for the values used for the polydispersities. The values obtained for the surface coverage however are lower than the inserted values, while the deduced radius is near the inserted value.

The adsorption can be followed as a function of time with reasonable precision; two examples are given also in Figure 4 (using the Mie-based fits). The adsorption typically saturates at coverages of about 0.1. At the higher coverages, the effect of interactions and possible correlations between particles should be considered, which is difficult within the framework of the Mie-based formalism. An exact treatment is currently being developed.[25]

5. Conclusions

We see from the data presented here that the reflectivity of colloidal particles on a glass substrate is well described by a theory in which the particles are modeled as a noninteracting

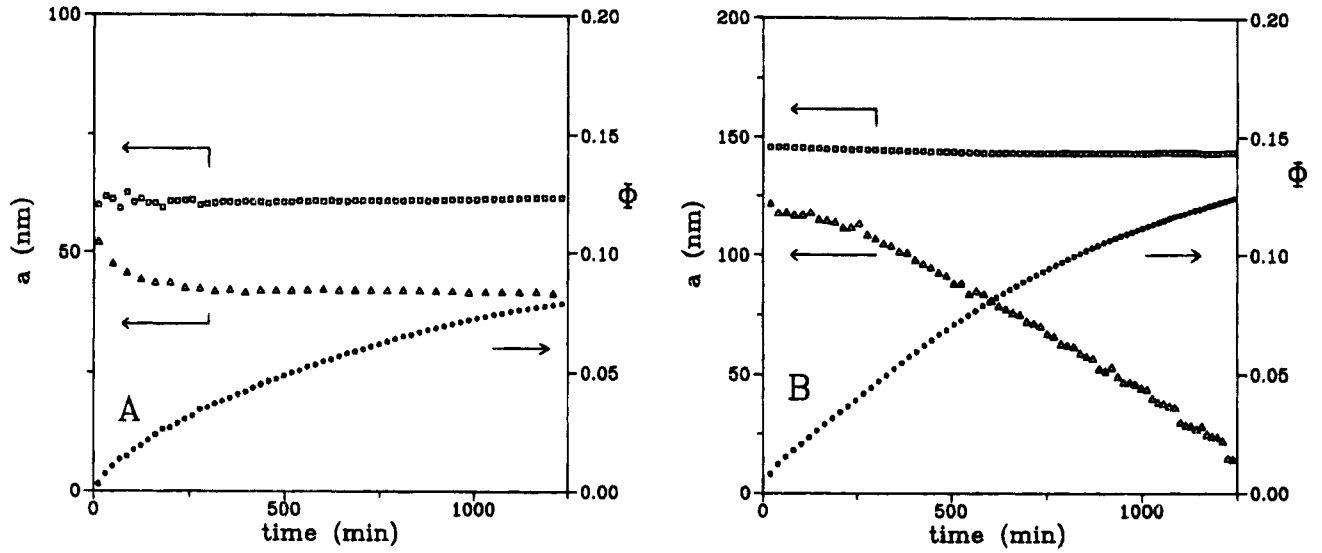

Figure 4. Radius of the 58 nm particles (A) and 150 nm particles (B) deduced from eq 2.9 (□) and eq 2.10 (△). The coverage (●) was deduced from eq 2.9.

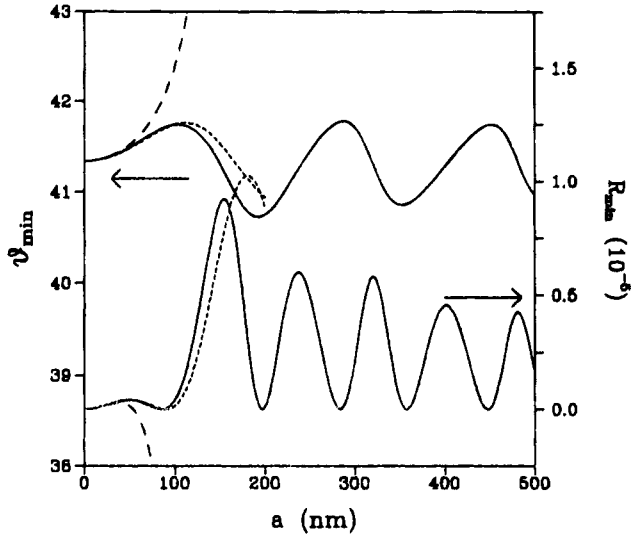

Figure 5. The intensity and angular position of the reflectivity minimum for a surface covered with dielectric spheres, as a function of particle radius a, assuming $n_1 = 1.5151$, $n_2 = 1.333$, $n_3 = 1.591$, and surface coverage $\varphi = 0.03$. Solid lines: deduced from eqs 2.9 and 2.4. Dotted lines: deduced from eqs 2.9 , 2.10, and 2.11. Dashed lines: deduced from eqs 2.12, 2.13, and 2.11.

plane of spheres, with the light scattered from each sphere given by Mie theory, ignoring direct interactions between the spheres and the interface.

This model can be linked to the Bedeaux/Vlieger formulation of the reflectivity of thin, inhomogeneous films, in which interactions between the spheres and the substrate can be taken into account. This theory, valid for particle radii $a \ll \lambda$, is at the limit of its applicability in the size range considered here, but it can be used to roughly describe the data for $a < 70$ nm. Since we have shown that the Mie and Bedeaux/Vlieger formulas are analytically equivalent for small sizes ($a < 20$ nm) and low densities, the good agreement of the data with Mie theory in the entire range explored suggests that both should hold for the smaller spheres.

Finally, we have demonstrated that it is possible to follow the particle surface coverage with exposure time; the application of this technique to adsorption processes is in progress. It is also seen that polydispersity mainly causes an underestimation of the coverage.

Acknowledgment. It is a pleasure to thank M. T. Haarmans, M. M. Wind, and J. Vlieger for many illuminating discussions on the use of optical theory. We also thank J. P. M. van de Ploeg, G. H. van Veen, H. Verpoorten, W. J. Jesse, and G. Maenel for technical support. The authors are grateful for financial support from the Région Alsace, DRET Contract 931099/A000, the Netherlands' Technology Foundation (STW), and the EEC (Contract SC1*-CT91-0696 (TSTS)).

Appendix

In the text, we develop a theory for the light reflected from an uncorrelated assembly of homogeneous dielectric spheres at an interface. To calculate this, we need to evaluate the scattering function due to a single sphere. In this appendix we give both the explicit form of the scattering function and the algorithms needed to calculate these with sufficient accuracy.

The general theory of light scattering by spheres was given by Mie in 1908.[6,7] The solution can be written in terms of two amplitude functions, one for p-polarized light,

$$S_p(\theta) = \sum_{l=1}^{\infty} \frac{2l+1}{l(l+1)} \left\{ a_l \frac{dP_l^1(\cos\theta)}{d\theta} + b_l \frac{P_l^1(\cos\theta)}{\sin\theta} \right\} \quad \text{(A.1a)}$$

and one for s-polarized light,

$$S_s(\theta) = \sum_{l=1}^{\infty} \frac{2l+1}{l(l+1)} \left\{ a_l \frac{P_l^1(\cos\theta)}{\sin\theta} + b_l \frac{dP_l^1(\cos\theta)}{d\theta} \right\} \quad \text{(A.1b)}$$

where $P_l^m(z)$ are the associated Legendre functions of the first kind of degree l and or order m.[26] The coefficients a_l and b_l can be conveniently expressed in terms of angles α_l and β_l such that

$$a_l = \frac{\tan\alpha_l}{\tan\alpha_l - i} \text{ and } b_l = \frac{\tan\beta_l}{\tan\beta_l - i} \quad \text{(A.2)}$$

These angles, mainly introduced to avoid complex number manipulation, can be calculated by

$$\tan\alpha_l = -\frac{n_3\psi'_l(y)\,\psi_l(x) - n_2\psi_l(y)\,\psi'_l(x)}{n_3\psi'_l(y)\,\chi_l(x) - n_2\psi_l(y)\,\chi'_l(x)} \quad \text{(A.3a)}$$

and

$$\tan \beta_l = -\frac{n_2\psi'_l(y)\,\psi_l(x) - n_3\psi_l(y)\,\psi'_l(x)}{n_2\psi'_l(y)\,\chi_l(x) - n_3\psi_l(y)\,\chi'_l(x)} \quad \text{(A.3b)}$$

with $x = k_3a$ and $y = k_2a$. The Ricatti–Bessel functions Δ_l and χ_l are related to the spherical Bessel functions of the first kind, j_l, and of the second kind, y_l, by

$$\psi_l(z) = zj_l(z) \quad \text{and} \quad \chi_l(z) = zy_l(z) \quad \text{(A.4)}$$

Great care has to be taken during the numerical evaluation of the coefficients a_l and b_l. It is for this reason that the coefficients are expressed in terms of the Ricatti–Bessel functions. In this form the coefficients can be determined to any desired accuracy, if one follows simple guidelines,[26] summarized below.

The Ricatti–Bessel function χ_l may be calculated by a simple forward recurrence relation:

$$\chi_0(z) = \cos z, \quad \chi_1 = \frac{\cos z}{z} + \sin z, \quad \chi'_1(z) = \cos z\left(1 - \frac{1}{z^2}\right) - \frac{\sin z}{z}$$

$$\chi_l(z) = \frac{(2l-1)\chi_{l-1}(z)}{z} - \chi_{l-2}(z), \quad \chi'_l(z) = \frac{-l\chi_l(z)}{z} + \chi_{l-1}(z) \; (l \geq 2)$$

The Ricatti–Bessel function ψ_l on the other hand should be calculated by an inverse recurrence relation as follows:

$$j_M(z) = 0, \quad j_{M-1}(z) = 1, \quad j_l(z) = \frac{(2l+3)j_{l+1}(z)}{z} - j_{l+2}(z)$$

$$p_0(z) = \frac{\sin z}{zj_0(z)}$$

$$\psi_l(z) = zj_l(z)\,p_0(z), \quad \psi'_l(z) = -\frac{l\psi_l(z)}{z} + \psi_l(z)$$

The reverse recurrence method is based on the observation that ψ_l is proportional to zj_l, for l sufficiently less than M; the factor of proportionality p_0 is calculated from the ratio of ψ_l and zj_l, for $l = 0$. In practice, if the scattering function is calculated to order l_M, then $M = l_M + 5$ yields a generous degree of precision.

Finally, the functions $\pi(\cos\theta) = P_l^1(\cos\theta)/\sin\theta$ and $\tau(\cos\theta) = \mathrm{d}P_l^1(\cos\theta)/\mathrm{d}\theta$ can again be calculated by simple forward recurrence relations:

$$\pi_1(z) = 1, \quad \pi_2(z) = 3z, \quad \tau_1(z) = z$$

$$\tau_2 = 6z^2 - 3, \quad \pi_l(z) = \frac{(2l-1)z\pi_{l-1}(z) - l\pi_{l-2}(z)}{l-1}$$

$$\pi'_l(z) = (2l-1)\pi_{l-1}(z) + \pi'_{l-2}(z), \quad \tau_l(z) = z\pi_l(z) - (1-z^2)\pi'_l(z)$$

With these relations, the full scattering function $S_p(\theta)$ can be calculated to the desired degree of precision in a straightforward manner. For our system, polystyrene spheres in water ($n_2 = 1.333$, $n_3 = 1.591$, $\lambda = 632.8$ nm), $l_M = 10$ is sufficient to reach a precision of $10^{-10}S_p(\theta)$ for spheres of radii $a < 250$ nm; it would be necessary to increase this value to $l_{max} = 17$ to reach this precision for $a = 500$ nm.

B. The Local Field and the Reflection Coefficient. For particles in a plane the local field is the sum of the incident field $\mathbf{E}_i$ and the fields originating from scattering by all other particles, $\mathbf{E}_s$. We take the plane of incidence as the xz plane; therefore, we don't have to consider the y component of the electric field. We shall solve the problem in the dipole limit; that is, the particles are small compared to the wavelength. They may then be characterized simply by their polarizability α.

According to the definition of the local field just given, we can write for the induced dipole moment of a particle at position $\mathbf{r}$

$$\mathbf{p}(\mathbf{r}) = \epsilon_0\boldsymbol{\alpha}\cdot\mathbf{E}_{los}(\mathbf{r}) = \epsilon_0\begin{pmatrix}\alpha_{||} & 0\\ 0 & \alpha_\perp\end{pmatrix}\cdot\mathbf{E}_{loc}(\mathbf{r}) \equiv \epsilon_0\tilde{\boldsymbol{\alpha}}\cdot\mathbf{E}_i(\mathbf{r}) \quad \text{(B.1)}$$

where $\mathbf{E}_{loc}(\mathbf{r})$ is the local field experienced by a particle at position $\mathbf{r}$, and $\boldsymbol{\alpha}$ the polarizability tensor. We shall call $\tilde{\boldsymbol{\alpha}}$ the *effective* polarizability tensor.

Consider the local field at an arbitrary particle, choosing the origin $\mathcal{O}$ to lie at this point. Assuming a homogeneous distribution of particles on the surface, we can relate the local field at $\mathbf{r}$ to the local field at $\mathbf{0}$ by

$$\mathbf{E}_{loc}(\mathbf{r}) = \mathbf{E}_{loc}(\mathbf{0})\exp(i\mathbf{k}_{||}\cdot\mathbf{r}) \quad \text{(B.2)}$$

with $\mathbf{k}_{||}$ the projection of the wave vector onto the interface.

The electric field at the origin originating from dipole j at position $\mathbf{r}$ is given by[27]

$$\mathbf{E}_j(\mathbf{r}) = \left(\frac{k^2}{r}(\mathbf{n}\times\mathbf{p})\times\mathbf{n} + \left\{\frac{1}{r^3} - \frac{ik}{r^2}\right\}(3\mathbf{n}(\mathbf{n}\cdot\mathbf{p}) - \mathbf{p})\right)\frac{e^{ikr}}{4\pi n_2{}^2\epsilon_0} \quad \text{(B.3)}$$

Here $\mathbf{n} \equiv \mathbf{r}/r$, k is the wavenumber of the light in the medium, and $\mathbf{p}$ is given by eq B.1. It is noted that in the far-field limit, the last two terms are negligible compared to the first. If we now substitute eq B.2 together with eq B.1 into eq B.3, we may define a tensor $\mathbf{T}$ by

$$\mathbf{E}_j(\mathbf{r}) = \boldsymbol{\alpha}\cdot\mathbf{T}\cdot\mathbf{E}_{lo}c(\mathbf{0}) \quad \text{(B.4)}$$

If we now sum up the contributions from all the dipoles and use the definition of the local field $\mathbf{E}_{loc}$, we get

$$\mathbf{E}_{loc}(\mathbf{0}) = \mathbf{E}_i(\mathbf{0}) + \varrho\boldsymbol{\alpha}\cdot\int g(r)\,\mathbf{T}(\mathbf{r})\cdot\mathbf{E}_{loc}(\mathbf{0})\,\mathrm{d}\mathbf{r} \quad \text{(B.5)}$$

with ϱ the average particle density (which is related to the coverage by $\varrho = \phi/\pi a^2$), and $g(r)$ the probability function of finding a particle at r, given a particle at $\mathbf{0}$. Assuming uncorrelated particles, we can easily see that this probability function is given by

$$g(r) = \begin{cases}0 & r < b\\ 1 & r \geq b\end{cases} \quad \text{(B.6)}$$

with b the distance of closest approach of the particles. The integral in eq B.5 has been evaluated by Johner,[28]

$$\int g(r)\,\mathbf{T}(\mathbf{r})\,\mathrm{d}\mathbf{r} = \begin{pmatrix}\frac{1}{4bn^2} + \frac{i\pi}{\lambda n_2}\cos\theta & 0\\ 0 & -\frac{1}{2bn^2} + \frac{i\pi}{\lambda n_2}\frac{\sin^2\theta}{\cos\theta}\end{pmatrix} \quad \text{(B.7)}$$

with θ the incident angle to the plane. Using eq B.7 and eq

B.1, we can solve eq B.5 for $\mathbf{E}_{loc}$ to get

$$\tilde{\alpha} = \begin{pmatrix} \dfrac{\alpha_{\parallel}}{1 - \dfrac{\varrho\alpha_{\parallel}}{4bn_2^2} - \dfrac{i\pi\varrho\alpha_{\parallel}}{\lambda n_2}\cos\theta} & 0 \\ 0 & \dfrac{\alpha_{\perp}}{1 + \dfrac{\varrho\alpha_{\perp}}{2bn_2^2} - \dfrac{i\pi\varrho\alpha_{\perp}}{\lambda n_2}\dfrac{\sin^2\theta}{\cos\theta}} \end{pmatrix} \quad \text{(B.8)}$$

Taking the static limit of the different components of the tensor $\tilde{\alpha}$, we can define

$$\alpha_{\parallel}^{stat} \equiv \frac{\alpha_{\parallel}}{1 - \dfrac{\varrho\alpha_{\parallel}}{4bn^2}} \quad \text{(B.9)}$$

$$\alpha_{\perp}^{stat} \equiv \frac{\alpha_{\perp}}{1 + \dfrac{\varrho\alpha_{\perp}}{2bn^2}}$$

Now we can rewrite $\tilde{\alpha}$ as

$$\tilde{\alpha} = \begin{pmatrix} \dfrac{\alpha_{\parallel}^{stat}}{1 + \dfrac{i\pi\varrho\alpha_{\parallel}^{stat}}{\lambda n_2}\cos\theta} & 0 \\ 0 & \dfrac{\alpha_{\perp}^{stat}}{1 - \dfrac{i\pi\varrho\alpha_{\perp}^{stat}}{\lambda n_2}\dfrac{\sin^2\theta}{\cos\theta}} \end{pmatrix} = \begin{pmatrix} \tilde{\alpha}_{\parallel} & 0 \\ 0 & \tilde{\alpha}_{\perp} \end{pmatrix} \quad \text{(B.10)}$$

If we use eq B.1 together with eq B.3, we obtain in the far-field limit

$$\mathbf{E}_j(\mathbf{r}) = \frac{-k^2}{4\pi n_2^2}\frac{e^{ikr}}{r}(\tilde{\alpha}_{\parallel}\cos^2\theta_2 - \tilde{\alpha}_{\perp}\sin^2\theta_2)\begin{pmatrix}\cos\theta_2 \\ \sin\theta_2\end{pmatrix} \quad \text{(B.11)}$$

If we now sum over all particles in the plane we get, following the analysis of Bobbert:[29]

$$r_l = -i\frac{\pi}{2\lambda}\frac{\varrho}{n_2}\left(\tilde{\alpha}_{\parallel}\cos\theta - \frac{\tilde{\alpha}_{\perp}\sin^2\theta}{\cos\theta}\right) \quad \text{(B.12)}$$

Defining γ and β as $\gamma = \varrho\alpha_{\parallel}^{stat}$ and $\beta = \varrho\alpha_{\perp}^{stat}/n_2^4$, this is exactly equivalent to expression 2.10.

Haarmans et al.[17] have analyzed the problem of the response of an assembly of spheres, taking into account the interaction with the substrate. Our expressions for γ and β are consistent with theirs, in the limit where the refractive indices of the substrate, medium, and particles are close.

C. Optical Invariants. The "invariant" form for the reflectivity was derived through a multipole expansion in which the surface excess polarizabilities were assumed to lie at a Fresnel interface. The reflectivity cannot depend on the choice of the position of this interface, and thus only certain combinations of the polarizabilities, invariant with respect to this choice, can appear. The first-order term can be seen trivially, following Bedeaux.[23]

In our case, consider the excess polarization for two different choices of this interface: one at the original Fresnel interface and one at a position d below it. Since the polarization of a homogeneous medium is given by $\mathbf{P} = (\epsilon - \epsilon_0)\mathbf{E} = (1 - \epsilon_0/\epsilon)\mathbf{D}$, the excess polarizability density parallel to the plane is given, in function of d, by

$$P_{\parallel}(d) - \gamma(d)\epsilon_0 E_{\parallel} = \left(\gamma(0) + \frac{\epsilon_1 - \epsilon_2}{\epsilon_0}d\right)\epsilon_0 E_{\parallel} \quad \text{(C.1)}$$

or

$$\gamma(d) = \gamma(0) + \frac{\epsilon_1 - \epsilon_2}{\epsilon_0}d \quad \text{(C.2)}$$

For the excess polarizability density perpendicular to the surface, one must use the dielectric displacement field $\mathbf{D}$:

$$P_{\perp}(d) = \beta(d)D_{\perp} = \left(\beta(0) - \left(\frac{1}{\epsilon_1} - \frac{1}{\epsilon_2}\right)\epsilon_0 d\right)D_{\perp} \quad \text{(C.3)}$$

We readily see that $\gamma - (\epsilon_1\epsilon_2/\epsilon_0^2)\beta$ is the first-order invariant combination of these polarizabilities; J_{21} and J_{22} are simply extentions to second order.

References and Notes

(1) Evans, J. W. *Rev. Mod. Phys.* **1993**, *65*, 1281.
(2) Adamczyk, Z.; Siwek, B.; Zembala, M. *Langmuir* **1992**, *8*, 2605.
(3) Adamczyk, Z.; Siwek, B.; Zembala, M.; Belouschek, P. *Adv. Colloid Interface Sci.* **1994**, *48*, 151.
(4) Wojtaszcyk, P.; Schaaf, P.; Senger, B.; Zembala, M.; Voegel, J. C. *J. Chem. Phys.* **1993**, *99*, 7198.
(5) Schaaf, P.; Déjardin, Ph.; Schmitt, A. *Ref. Phys. Appl.* **1986**, *21*, 741.
(6) Hulst, van de H. C. *Light Scattering by Small Particles*; Dover: New York, 1981.
(7) Kerker, M. *The scattering of light and other electromagnetic radiation*; Academic Press: New York, 1969.
(8) Berreman, D. W. *Phys. Rev.* **1967**, *163*, 855.
(9) Chauvaux, R.; Meessen, A. *Thin Solid Films* **1979**, *62*, 1125.
(10) Ruppin, R. *Surf. Sci.* **1983**, *127*, 108.
(11) Wind, M. M.; Vlieger, J.; Bedeaux, D. *Physica A* **1987**, *141*, 33.
(12) Wind, M. M.; Bobbert, P. A.; Vlieger, J.; Bedeaux, D. *Physica A* **1987**, *143*, 164.
(13) Bobbert, P. A.; Vlieger, J. *Physica A* **1987**, *147*, 115.
(14) Bobbert, P. A.; Vlieger, J. *Physica A* **1986**, *137*, 209.
(15) Bobbert, P. A.; Vlieger, J. *Physica A* **1986**, *137*, 243.
(16) Vlieger, J.; Bedeaux, D. *Thin Solid Films* **1980**, *69*, 107.
(17) Haarmans, M. T.; Bedeaux, D. *Thin Solid Films* **1993**, *224*, 117.
(18) Haarmanx, M. T.; Bedeaux, D. *Physica A* **1994**, *207*, 340.
(19) Greef, R. *Ber. Bunsen-Ges. Phys. Chem.* **1984**, *88*, 150.
(20) Azzam, R. M. A.; Bashara, N. M. *Ellipsometry and Polarized Light*; North Holland Publishing Co.: Amsterdam, 1989.
(21) Koper, G. J. M.; Schaaf, P. *Europhys. Lett.* **1993**, *22*, 543.
(22) The paper by Koper and Schaaf[21] considers the situation in which the area of the layer illuminated by the light beam is small compared to the area from which the nondestructively interfering contributions at the observation site originate. They wrongly conclude that this corresponds to the experimental situation and use an erroneous expression for eq 2.9. In particular this leads to a wrong phase factor between the scattered light and the Fresnel field as well as to coefficients (c_1 and c_2) in front of the interference term and the scattering term, respectively; see eq 4.1.
(23) Bedeaux, D.; Koper, G. J. M.; Zeeuw, van der E. A.; Vlieger, J.; Wine, M. M. *Physica A* **1994**, *207*, 285.
(24) Lekner, J. *Theory of Reflection*; Martinus Nijhoff Publishers: Dordrecht, 1987.
(25) Haarmans, M. T. Personal communication.
(26) Abramowitz, M.; Stegun, I. A. *Handbook of Mathematical Functions*; Dover: New York, 1972; p 452.
(27) Jackson, J. D. *Classical Electrodynamics*; Wiley: New York, 1975; p 395.
(28) Johner, A. Ph.D. Thesis, Université Louis Pasteur de Strasbourg, 1988; pp 97, 98.
(29) Bobbert, P. A. Ph.D. Thesis, Leiden, 1986.

JP942203D